

# Chapter 20

## Numerical Investigation on Combustion Characteristics and NO<sub>x</sub> Emission of Double-Reheat Tower Boiler at Different Loads



Yan Zhang, Shihao Ma, Jin Guo, Yuesheng Li, Zhengrong Zhu, Jiaqi He, Lei Deng, and Defu Che

**Abstract** In this study, a three-dimensional numerical investigation using a finite volume method is presented to obtain the velocity, temperature, and species distributions in a 660 MW double-reheat tower boiler fed with bituminous coal. The refined oxidation model of HCN and NO-char reaction model were used to substitute the default model by the user-defined functions (UDFs). The effects of different loads and excess air ratios on combustion characteristics and NO<sub>x</sub> emission were studied numerically. The results show that temperature distribution is more uneven at the upper part of the furnace and the NO<sub>x</sub> emission increases as the load decreases. The temperature distributions in the furnace have little differences under three different excess air ratios. That the oxygen concentration increases significantly as the increase of excess air ratios leads to an increase of NO<sub>x</sub> emission at the furnace outlet. The minimum NO<sub>x</sub> concentration at the furnace outlet, 308 ppm, appears under 100% THA with excess air ratio of 1.15. The simulation results in this study can provide reference for optimization of combustion characteristics in double-reheat tower boiler and illustrate a method to reduce NO<sub>x</sub> emission.

**Keywords** Unit load · Excess air ratio · NO<sub>x</sub> emission · Double-reheat · Numerical investigation

---

Y. Zhang · S. Ma · Z. Zhu · J. He · L. Deng (✉) · D. Che  
State Key Laboratory of Multiphase Flow in Power Engineering, School of Energy and Power Engineering, Xi'an Jiaotong University, Xi'an 710049, China  
e-mail: [leideng@mail.xjtu.edu.cn](mailto:leideng@mail.xjtu.edu.cn)

J. Guo  
Guangdong Institute of Special Equipment and Research, Foshan 528251, China

Y. Li  
Guangdong Institute of Special Equipment Inspection and Research, Shunde Institute of Inspection, Foshan 528300, China

## 20.1 Introduction

With the slowdown of economic growth and the rapid adjustment of the economic structure, China's overall electricity demand has declined. The contradiction between power supply and demand has shifted from electricity shortage to relative surplus. Meanwhile, to face the increasingly severe environmental regulations, China continues to promote energy structure adjustment and develop the clean energy rapidly. These all lead to the decline of our country's installed capacity of thermal power units while moving toward the development of large-capacity and high-parameter double-reheat unit (Tumanovskii and Shvarts 2017; Chang and Zhuo 2016). Besides, conditions of medium and low loads would become more universal during the unit operations due to the abundant hydropower or low power demand in late nights (Zhao and Fang 2017). However, most of the units lack experiences of long-term operation under medium and low loads, which makes the efficiency of the units decrease and the coal consumption increase. Therefore, it is necessary to carry out investigation on energy-saving operation optimization of large-capacity and high-parameter double-reheat units under conditions of wide loads to improve the efficiency and reduce pollutant emissions and power consumption.

Ultra-supercritical double-reheat units with high efficiency, high parameter and large capacity have become a main development tendency on the coal-fired power plants. But double-reheat units are still in the initial development stage in China. Several researches have analyzed the technical (Huo and Shi 2014) and economic characteristics (Jiang 2000; Yao and Zhu 2017), heat load distribution (Zhang and Yan 2016) and pollutant control (Guo and Zhang 2011) during the operation of double-reheat units. However, the studies on ultra-supercritical double-reheat units are still limited.

Numerical simulation, which has been widely applied to investigate the combustion and pollutant formation process in pulverized coal fired boiler in the past few decades (Zhou and Mo 2011; Liu and Chen 2015), is more economical and convenient than experimental study. In this study, the effects of different loads and excess air ratios on combustion characteristics and  $\text{NO}_x$  emission of an ultra-supercritical double-reheat boiler were studied. In  $\text{NO}_x$  calculation, the revised  $\text{NO}_x$  model is used to replace the default model to accurately predict the  $\text{NO}_x$  emission. This work can provide reference for optimization of combustion organization for double-reheat tower boiler.

## 20.2 Boiler Description

The simulations were based on a 660 MW double reheat tower boiler with bituminous coal, with the schematic of boiler geometry illustrates in Fig. 20.1a. The width, depth and height of the boiler are 18,150, 18,150 and 97,500 mm, respectively. Figure 20.1b shows the arrangement of nozzles in each corners. It includes the primary air (PA),

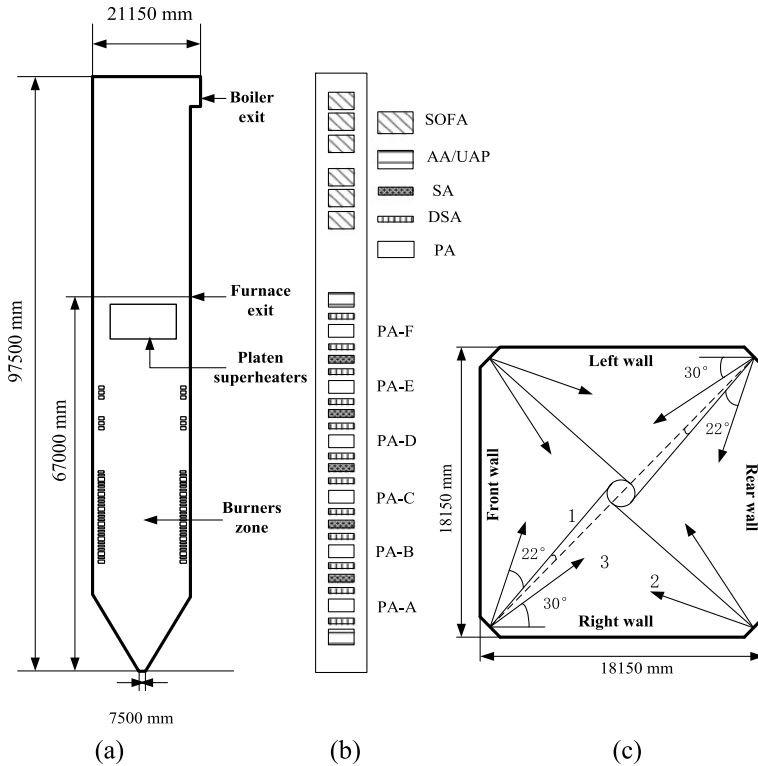


**Fig. 20.1** Schematic configuration and burner nozzle distribution of the tangentially pulverized coal fired boiler

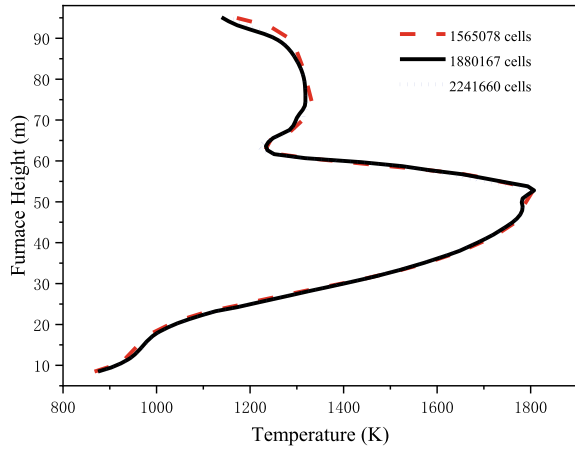
secondary air (SA) and separate over fire air (SOFA). In order to control the  $NO_x$  generation by air staging, two stage SOFA nozzles are arranged above the burners. Figure 20.1c presents the air injecting direction.

### 20.3 Modeling Methodology

#### 20.3.1 Grid Independence

In this paper, a structured grid is used to simulate the coal combustion. Because of the intense combustion reaction in the burner area, the grid is refined locally to receive more accurate results in this area. The grid independence was verified with three different mesh systems, i.e., 1,565,078, 1,880,167 and 2,241,660 cells. Figure 20.2 depicts the temperature distribution in the three different mesh systems.

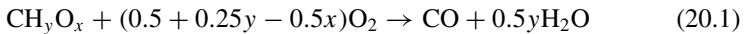
**Fig. 20.2** Grid independence



By comparing the simulation results, the mesh with 1,880,167 cells is chosen to calculate.

### 20.3.2 Numerical Models

The combustion process of pulverized coal furnace includes a series of complex physical and chemical processes (Hu and Liu 2013). The standard  $k - \varepsilon$  model was chosen in the present study. The radiation heat transfer was calculated by P-1 model (Drosatos and Nikolopoulos 2015). The WSGGM-domain based model was used to calculate the gas absorption coefficient. The volatile combustion is described by the two-step global reaction mechanism as follow. Coal particle trajectories were calculated using the Lagrangian approach.



The NO is generally discussed when investigating  $\text{NO}_x$  formation in coal-fired boilers. That's because the NO accounts for 95% of total  $\text{NO}_x$ . Three types of  $\text{NO}_x$  are generated, named as prompt  $\text{NO}_x$ , thermal  $\text{NO}_x$  and fuel  $\text{NO}_x$ . In large pulverized coal combustion system, the prompt  $\text{NO}_x$  production is little, which is generally neglected (Panagiotis and Athanasios 2016; Álvarez and Yin 2013). Thus, only thermal  $\text{NO}_x$  and fuel  $\text{NO}_x$  are taken into consideration in the calculation process.  $\text{NO}_x$  generation is calculated by post-processing method (Park 2013).

The generation and reduction of thermal  $\text{NO}_x$  are determined by the extended Zeldovich mechanism as follows:



where  $k_1, k_2, k_3$  present the forward reaction rate constant, while  $k_{-1}, k_{-2}, k_{-3}$  present the reverse reaction rate constant in the Eqs. (20.3–20.5). The six reaction rate constants are determined by the experimental results acquired by Hanson. Thus, the thermal NO formation rate can be described as the Eqs. (20.6). Besides, the concentrations of O, H, and OH in the Eqs. (20.3–20.6) are computed by the partial equilibrium approach.

$$\begin{aligned} \frac{d[\text{NO}]}{dt} = & k_1[\text{O}][\text{N}_2] + k_2[\text{N}][\text{O}_2] + k_3[\text{N}][\text{OH}] \\ & - k_{-1}[\text{NO}][\text{N}] - k_{-2}[\text{NO}][\text{O}] - k_{-3}[\text{NO}][\text{H}] \end{aligned} \quad (20.6)$$

Fuel  $\text{NO}_x$  is usually released in the form of volatile nitrogen and char nitrogen. Char nitrogen is converted to NO directly. During the transformation process from volatile nitrogen to the fuel  $\text{NO}_x$ , volatile nitrogen is first converted to HCN and  $\text{NH}_3$ , and then oxidation and reduction reactions occur between HCN,  $\text{NH}_3$  and NO,  $\text{O}_2$ , depicted as the Eqs. (20.7–20.10).



In this study, the User Defined Functions (UDF) was used to substitute the default models for  $\text{NO}_x$  calculation, which has been verified by Zhang and Ito (2013) and Zha and Li (2017). Surface reaction of  $\text{NO}_x$  reduction by char nitrogen was calculated according to Levy and Chana (1981) mechanism.

The properties of the bituminous coal are presented in Table 20.1. The basic simulation case is based on the design case of 100% turbine heat acceptance (THA) operation. The effect of different unit loads and excess air ratios on the characteristics of  $\text{NO}_x$  emission are considered to study in the work. The three loads are 100% THA, 70% THA and 50% THA with the total excess air ratio of 1.15. The three excess air

**Table 20.1** Basic information of the bituminous coal

Proximate analysis (ar, %)		Ultimate analysis (daf, %)	
$w(V)$	25.02	$w(C)$	78.86
$w(FC)$	43.62	$w(H)$	5.62
$w(A)$	14.96	$w(O)$	12.60
$w(M)$	16.40	$w(N)$	2.20
		$w(S)$	0.72
$Q_{net}$ (MJ/kg)		20.36	

**Table 20.2** Simulation cases of the 660 MW tower boiler

Case	Loads	Excess air ratios	Coal mills
Case 1	100% THA	1.15	A-E
Case 2	70% THA	1.15	B-E
Case 3	50% THA	1.15	C-E
Case 4	100% THA	1.20	A-E
Case 5	100% THA	1.25	A-E

ratios are 1.15, 1.20 and 1.25 with 100% THA load. All detailed simulation cases are listed in Table 20.2.

## 20.4 Results and Discussion

### 20.4.1 Validation of the CFD simulation

In order to obtain credible and reasonable simulation results, the numerical calculation results were verified by the thermal calculation values with three different loads. Table 20.3 shows the comparison between the CFD results and thermal calculated value of furnace outlet temperature. The maximum deviation between the CFD results and thermal calculated value is 18 K under 100% THA operation.

**Table 20.3** Comparison of furnace outlet temperature (K) between CFD results and thermal calculated value

Load	Excess air ratios	CFD	Thermal calculated
100% THA	1.15	1208	1226
70% THA	1.15	1146	1139
50% THA	1.20	1059	1074

### 20.4.2 Effects of Different Unit Loads on the Combustion Characteristics and $NO_x$ Emission

Figure 20.3 shows the temperature distribution along furnace height under different unit loads. The coal quantity decreases with the load decrease. This results in reduction of the temperature level in the furnace. Besides, both the amount of pulverized coal and air are reduced, which leads to a decreasing gas fullness in the furnace. It can be seen from Fig. 20.3 that under the condition of 50% THA load, the temperature distribution at the upper part of the furnace is uneven. This can be explained by that the low gas fullness under the condition of 50% THA load results in the uneven velocity distribution in the furnace. Thus, heat exchanges between the gas and wall are different in different positions, which eventually leads to uneven temperature distribution at the upper part of the furnace. The temperature distribution showed a similar tendency with the results of Liu and Zhang (2019).

Figure 20.4 presents the average temperature on furnace cross-section along the height direction under different loads. The temperature distribution is similar under three boiler loads, while combustion details are different in the main combustion zone ranging from 24 to 41 m. In the main combustion zone, the temperature has a sharp decrease due to the injection of a large amount of primary air with the lower temperature. For the 50% THA load, that coal mills A-B in the lower position are closed causes that the temperature sharp decrease occurs in a higher position when compared with the 100% THA load and the 70% THA load. There is another sharp temperature decrease resulted from the injection of SOFA in the burnout zone. It is evident that the area-weighted average temperature at the furnace outlet  $T_{av}$  decreases as  $T_{av}(100\% \text{ THA}) > T_{av}(70\% \text{ THA}) > T_{av}(50\% \text{ THA})$  with the highest temperature appearing at 100% THA load.

**Fig. 20.3** Temperature distribution along the height direction under different loads

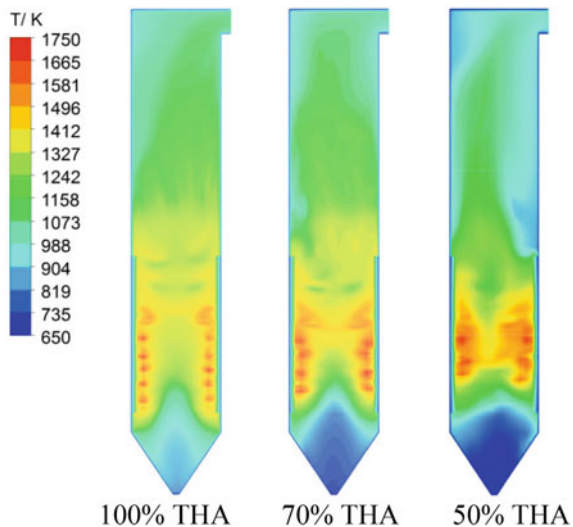


**Fig. 20.4** Area-weighted average temperature along the height direction under different loads

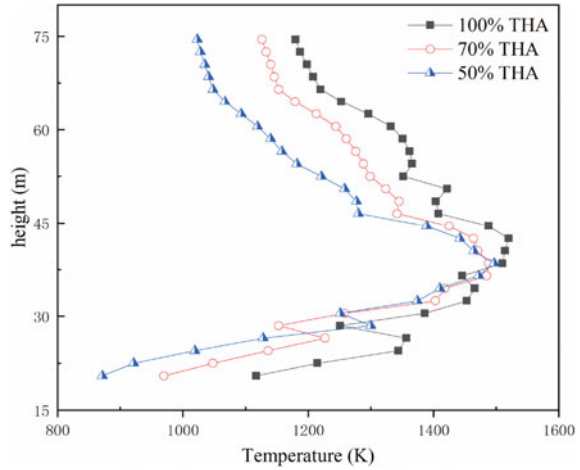
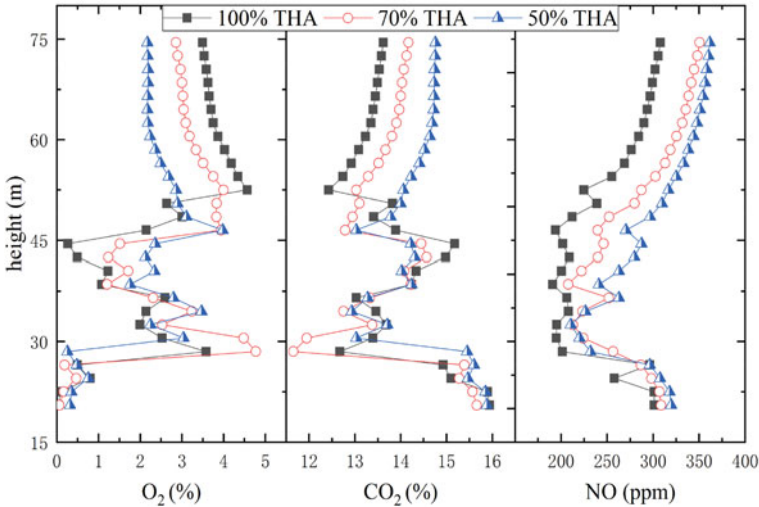


Figure 20.5 shows area-weighted average species distribution along the height direction under different loads. With the injection of the air and the combustion reaction, the  $O_2$  concentration  $C_{O_2}$  changes drastically in the combustion zone. As shown in Fig. 20.5, the area-weighted average  $O_2$  concentration at the furnace outlet  $C_{O_2}$  descends as  $C_{O_2}$  (100% THA) >  $C_{O_2}$  (70% THA) >  $C_{O_2}$  (50% THA). During the combustion of the furnace, most of  $O_2$  is consumed to generate  $CO_2$ . The  $C_{CO_2}$  decreases with the increasing loads as  $C_{CO_2}$  (50% THA) >  $C_{CO_2}$  (70% THA) >  $C_{CO_2}$  (100% THA) with the highest  $C_{CO_2}$  appearing at the 50-THA load. In the furnace



**Fig. 20.5** Area-weighted average species distribution along the height direction under different loads



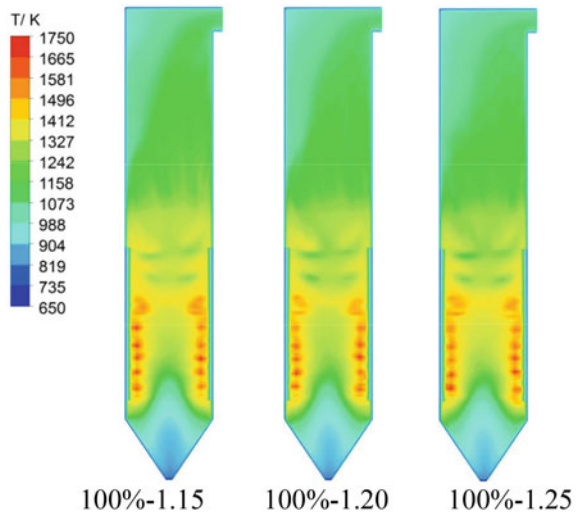
outlet, it is obviously seen that NO concentration decreases with increased loads as  $C_{NO} (50\% \text{ THA}) > C_{NO} (70\% \text{ THA}) > C_{NO} (100\% \text{ THA})$ . So it can be concluded that  $NO_x$  concentrations in the flue gas often increases obviously with the decrease of the boiler operating load, which is consistent with the results of Zheng (Yang and Gao 2017).

### 20.4.3 Effects of Different Excess Air Ratios on the Combustion Characteristics and $NO_x$ Emission

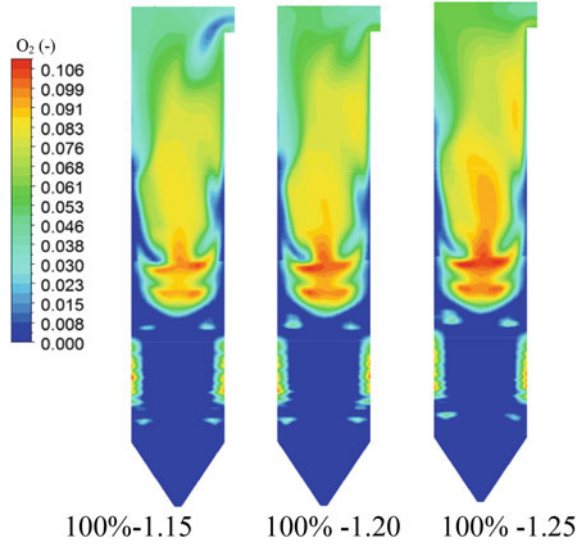
Temperature distributions along the height direction at different excess air ratios are demonstrated as Fig. 20.6. The combustion reaction near the nozzles in the main combustion zone is severe and the average temperature of the furnace gradually increases along the height of the furnace. After the overfire air with lower temperature is injected, the temperature in the furnace is reduced, while a small amount of heat is released as the char combustion. Above the main combustion zone, due to the heat exchange with water-cooled walls and superheater, the gas temperature begins to decrease. Under the three conditions of different excess air ratios, the temperature distributions in the furnace have little differences. This is because the oxygen concentration in the main combustion zone increases as the excess air ratio increases, which leads to that the combustion reaction in the main combustion zone is fully carried out and releases more heat. On the other hand, to heat the air with lower temperature causes the furnace temperature to decrease.

Figure 20.7 shows the  $O_2$  distribution under different excess air ratios. As the excess air ratio increases, the oxygen concentration above the overfire air nozzles

**Fig. 20.6** Temperature distribution along the height direction at different excess air ratios

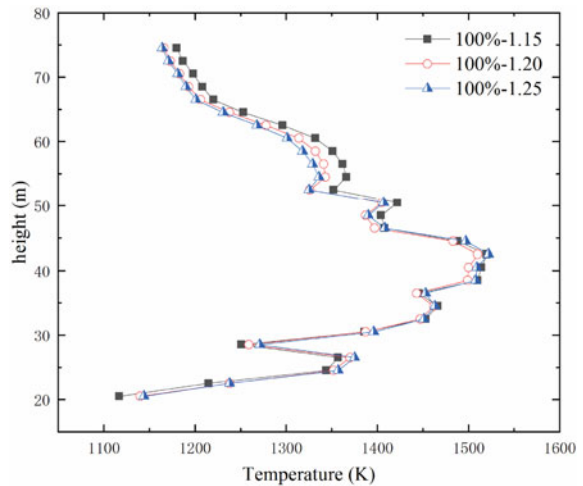


**Fig. 20.7** O<sub>2</sub> distribution along the height direction under different excess air ratios



increases significantly. Figure 20.8 shows area-weighted average temperature and species distribution along the height direction under different air ratios. It can be seen from the Fig. 20.9 that the oxygen concentration is smaller in the main combustion zone. This is because the boiler adopts air-staging combustion technology, and the excess air ratio in the main combustion zone is less than 1.0, forming a strong reductive atmosphere, and the combustion reaction is insufficient. As the excess air ratio increases, the amount of oxygen concentration in the main combustion zone increases and combustion reaction in the furnace is more sufficient, so the high

**Fig. 20.8** Area-weighted average temperature along the height direction under different excess air ratios



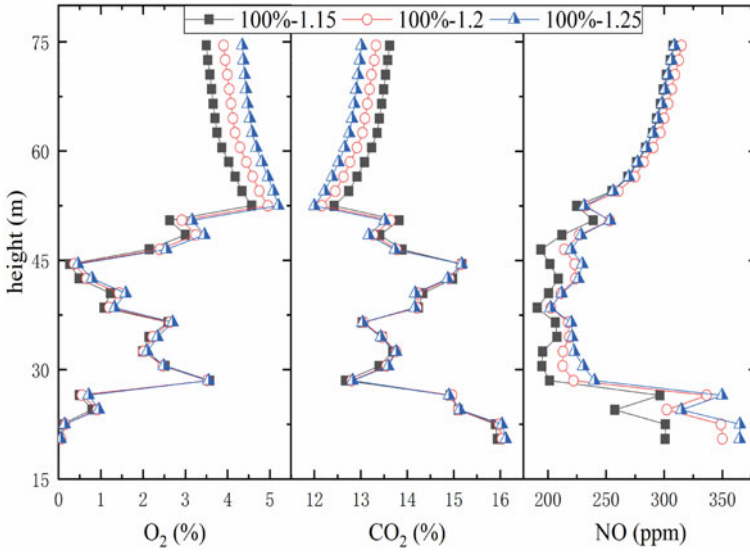


**Fig. 20.9** Area-weighted average species distribution along the height direction under different excess air ratios

temperature region in the furnace gradually expands. With the injection of SOFA, the oxygen concentration increases significantly, and the char has almost burned out, so that the increase of excess air ratio will lead to an increase in NO<sub>x</sub> emissions at the furnace outlet.

## 20.5 Conclusions

In this study, the effects of different loads and excess air ratios on combustion characteristics were studied by numerical simulation in an ultra-supercritical double-reheat unit. In NO<sub>x</sub> calculation, the revised NO<sub>x</sub> model is applied to replace the default model to accurately predict NO<sub>x</sub> emission. The following conclusions are obtained:

1. As the load decreases, velocity distribution in the furnace are more uneven, which leads to more uneven temperature distribution at the upper part of the furnace. The NO<sub>x</sub> emission increases while the boiler operates under the low and medium loads.
2. Under three conditions of different excess air ratios, the temperature distributions in the furnace have little differences. With the injection of SOFA, the oxygen concentration increases significantly, and the char has almost burned out, so that the increase of excess air ratios will lead to an increase in NO<sub>x</sub> emission at the furnace outlet.

3. In the five simulation cases of the 660 MW tower boiler, the minimum NO<sub>x</sub> concentration at the furnace outlet is 308 ppm, appearing under 100% THA with excess air ratio of 1.15.

**Acknowledgements** This work was supported by the National Key R&D Program of China (2017YFB0602102).

## References

- Álvarez L, Yin C (2013) Oxy-coal combustion in an entrained flow reactor: application of specific char and volatile combustion and radiation models for oxy-firing conditions. *Energy* 62(6):255–268
- Chang S, Zhuo J (2016) Clean coal technologies in China: current status and future perspectives. *Engineering* 2(4):447–459
- Drosatos P, Nikolopoulos N (2015) Numerical investigation of firing concepts for a flexible Greek lignite-fired power plant. *Fuel Process Technol* 142(2):370–395
- Guo Z, Zhang S (2011) The pure heat conversion coefficient analysis method for thermal system in supercritical pressure power unit with double reheat cycles 2011
- Hu L, Liu Y (2013) Effects of air staging conditions on the combustion and NO<sub>x</sub> emission characteristics in a 600 MW wall fired utility boiler using lean coal. *Energy Fuels* 27(10):5831–5840
- Huo H, Shi Q (2014) Influence of piping thermal efficiency on thermal economy of a 1000 MW double reheat power unit. *J Chinese Soc Power Eng*
- Jiang D (2015) 1000 MW supercritical double reheat boiler technology. *Value Eng*
- Levy JM, Chana LK (1981) NO/Char reactions at pulverized coal flame conditions. *Symp Combust* 18(1):111–120
- Liu G, Chen Z (2015) Numerical simulations of flow, combustion characteristics, and NO<sub>x</sub> emission for down-fired boiler with different arch-supplied over-fire air ratios. *Appl Therm Eng* 75(1):1034–1045
- Liu H, Zhang L (2019) Effect of FGR position on the characteristics of combustion, emission and flue gas temperature deviation in a 1000 MW tower-type double-reheat boiler with deep-air-staging. *Fuel* 246:285–294
- Panagiotis D, Athanasios N (2016) Numerical investigation of NO<sub>x</sub> emissions for a flexible greek lignite-fired power plant. *J Energy Eng*
- Park, Young H (2013) Numerical and experimental investigations on the gas temperature deviation in a large scale, advanced low NO<sub>x</sub>, tangentially fired pulverized coal boiler. *Fuel* 104(2):641–646
- Tumanovskii AG, Shvarts AL (2017) Review of the coal-fired, over-supercritical and ultra-supercritical steam power plants. *Therm Eng* 64(2):83–96
- Yang Z, Gao X (2017) Impact of co-firing lean coal on NO<sub>x</sub> emission of a large-scale pulverized coal-fired utility boiler during partial load operation. *Korean J Chem Eng* 34(4):1–8
- Yao D, Zhu Y (2017) Design characteristics of 1000MW double reheat ultra-supercritical tower boiler. *Boiler Technol*
- Zha Q, Li D (2017) Numerical evaluation of heat transfer and NO<sub>x</sub> emissions under deep-air-staging conditions within a 600 MWe tangentially fired pulverized-coal boiler. *Appl Thermal Eng* 116:170–181
- Zhang J, Ito T (2013) Improvement of NO<sub>x</sub> formation model for pulverized coal combustion by increasing oxidation rate of HCN. *Fuel* 113(2):697–706
- Zhang W, Yan K (2016) Research on thermal hydrodynamic performance of water wall pipes for ultra-supercritical double reheat once-through boiler. *J Eng Thermal Energy Power* 31(8):75–80

- Zhao S, Fang Q (2017) New fuel air control strategy for reducing  $\text{NO}_x$  emissions from corner-fired utility boilers at medium-low loads. *Energy Fuels* 31(7):6689–6699
- Zhou H, Mo GY (2011) Numerical simulation of the  $\text{NO}_x$  emissions in a 1000 MW tangentially fired pulverized-coal boiler: influence of the multi-group arrangement of the separated over fire air. *Energy Fuels* 25(5):2004–2012